Registry No. $AuCl_4^-$, 14337-12-3; $AuBr_4^-$, 14337-14-5; $PtCl_4^{2-}$, 13965-91-8; $PtBr_4^{2-}$, 14493-01-7; $PdCl_4^{2-}$, 14349-67-8; $PdBr_4^{2-}$, 14127-70-9; ICl_4^-, 15392-46-8; ICl_2^-, 14522-79-3; $HgCl_2$, 7487-94-7; $HgBr_2$, 7789-47-1; HgI_2, 7774-29-0.

References and Notes

(1) L. A. Woodward and J. A. Creighton, *Spectrochim. Acta*, **17**, 594 (1961).
(2) L. A. Woodward and M. J. Ware, *Spectrochim. Acta*, **19**, 775 (1963).
(3) D. A. Long and E. L. Thomas, *Trans. Faraday Soc.*, **59**, 1026 (1963).
(4) Y. M. Bosworth and R. J. H. Clark, *J. Chem. Soc., Dalton Trans.*, 1749 (1974).
(5) T. V. Long and R. A. Plane, *J. Chem. Phys.*, **43**, 457 (1965).
(6) R. J. H. Clark and C. J. Willis, *Inorg. Chem.*, **10**, 1118 (1971).
(7) R. J. H. Clark and P. D. Mitchell, *J. Chem. Soc. Faraday Trans. 2*, **68**, 476 (1972).
(8) R. J. H. Clark and P. D. Mitchell, *J. Mol. Spectrosc.*, **51**, 458 (1974), and references therein.
(9) W. F. Murphy, W. Holzer, and H. J. Bernstein, *Appl. Spectrosc.*, **23**, 211 (1969), and references therein.
(10) R. J. H. Clark and D. M. Rippon, *J. Chem. Soc., Faraday Trans. 2*, **69**, 1496 (1973).
(11) R. J. H. Clark and P. D. Mitchell, *Inorg. Chem.*, **11**, 1439 (1972).
(12) P. Braunstein and R. J. H. Clark, *J. Chem. Soc., Dalton Trans.*, 1845 (1973).
(13) A. I. Popov and R. E. Buckles, *Inorg. Syn.*, **5**, 167 (1967).
(14) W. Kiefer and H. J. Bernstein, *Appl. Spectrosc.*, **25**, 501 (1971).
(15) R. J. H. Clark, *Spex Speaker*, **18**, 1 (1973).
(16) L. A. Woodward, *Raman Spectrosc.*, 1 (1967).
(17) G. W. Chantry and R. A. Plane, *J. Chem. Phys.*, **32**, 319 (1960).
(18) J. Behringer, *Raman Spectrosc.*, 168 (1967).
(19) A. C. Albrecht, *J. Chem. Phys.*, **33**, 156 (1960).
(20) A. C. Albrecht, *J. Chem. Phys.*, **34**, 1476 (1961).
(21) The symmetry species to which the electronic states e and s belong is E_u for molecules and ions of symmetry point group D_{4h}.
(22) W. L. Peticolas, L. Nafie, P. Stein, and B. Fanconi, *J. Chem. Phys.*, **52**, 1576 (1970).
(23) A. H. Kalantar, E. S. Franzosa, and K. K. Innes, *Chem. Phys. Lett.*, **17**, 335 (1972).
(24) M. Eliashevich and M. Wolkenstein, *J. Phys. U.S.S.R.*, **9**, 101, 326 (1945).
(25) G. W. Chantry in "The Raman Effect," A. Anderson, Ed., Marcel Dekker, New York, N. Y., 1971, p 49.
(26) R. P. Bell, *Trans. Faraday Soc.*, **38**, 422 (1942).
(27) R. P. Bell and D. A. Long, *Proc. Roy. Soc. Ser. A*, **203**, 364 (1950),
(28) The complete set of solutions for the ICl_4^- ion is given as follows by way of illustration.. For each solution, the order is $\alpha_\parallel{}'$, $\alpha_\perp{}'^{a}$, $\alpha_\perp{}'^{b}$: 6.9, 0.50, 0.39; 1.7, −4.7, −4.8; 4.7, −1.7, 4.8; −0.50, −6.9, −0.39; 0.50, 6.9, 0.39; −4.7, 1.7, −4.8; −1.7, 4.7, 4.8; −6.9, −0.50, −0.39.
(29) The excitation profile of the a_{1g} band of each of these ions looks like the inverse of the absorption band in the vicinity of the ligand field transitions. This effect has also been observed by V. Miskowski, W. H. Woodruff, J. P. Griffin, K. G. Werner, and T. G. Spiro, *J. Chem. Phys.*, submitted for publication.

Contribution from Research School of Chemistry, Australian National University,
Canaberra, A.C.T., Australia, and from Bell Laboratories Inc., Murray Hill, New Jersey

Electronic Absorption Spectra of Tetragonal and Pseudotetragonal Cobalt(II). I. K_2CoF_4, Rb_2CoF_4, $K_2Mg(Co)F_4$, and $Rb_2Mg(Co)F_4$

JAMES FERGUSON,*[1a] T. E. WOOD,[1a] and H. J. GUGGENHEIM[1b]

Received April 24, 1974 AIC40274+

The electronic absorption spectra of K_2CoF_4, Rb_2CoF_4, $K_2Mg(Co)F_4$, and $Rb_2Mg(Co)F_4$ have been measured in polarized light and at low temperatures. Analyses of all of the main spectral features have been made using the complete d^7 tetragonal spin–orbit matrices in the weak-field formalism. These analyses provide, unambiguously, the signs of Dt in every case and the sign of Ds for all but $K_2Mg(Co)F_4$. It is concluded that K_2CoF_4 ($Ds = 195\ cm^{-1}$, $Dt = 10\ cm^{-1}$), $Rb_2Mg(Co)F_4$ ($Ds = 230\ cm^{-1}$, $Dt = 20\ cm^{-1}$), and Rb_2CoF_4 ($Ds = 335\ cm^{-1}$, $Dt = 30\ cm^{-1}$) have axially elongated fluoride octahedra with the magnitude of the distortion increasing from K_2CoF_4 to Rb_2CoF_4. The distortion in $K_2Mg(Co)F_4$ ($|Ds| = 60\ cm^{-1}$, $Dt = -10\ cm^{-1}$) is an axial compression, in agreement with the known crystal structure of K_2MgF_4. The transitions to the components of $^4T_{2g}$ occur *via* magnetic and electric dipole mechanisms and it is probable that the detailed understanding of the spin–orbit structure of this state will require consideration of the dynamic Jahn–Teller effect.

Introduction

With the considerable increase in our understanding of the detailed properties of paramagnetic ions in exactly cubic environments, attention has turned in recent years to the optical and magnetic properties of compounds with symmetries lower than cubic. For a study of transition metal ions in sites of tetragonal symmetry, the series of fluorides crystallizing with the K_2NiF_4 structure represent highly attractive systems, since both the factor group symmetry and paramagnetic ion site symmetry are D_{4h}.

K_2CoF_4 and Rb_2CoF_4 have the K_2NiF_4 structure and both are two-dimensional antiferromagnets[2] whose magnetic properties have been studied extensively.[3-7] K_2MgF_4 and Rb_2MgF_4 also have the same structure and are ideal host crystals for Co^{2+} for use in spectroscopic studies.

There have been two reports of optical absorption measurements of K_2CoF_4. Tiwari, *et al.*,[8] reported the unpolarized room-temperature electronic absorption spectrum but failed to include in their analysis the tetragonal component of the crystal field. Maisch[9] extended this work by measuring the three possible polarized spectra at low temperatures. He was, however, unable to arrive at an unambiguous assignment, based on the tetragonal matrices of Jesson, although one of his alternatives gave closer agreement with the results of Folen, *et al.*[5]

The present paper presents the results of a spectroscopic study of the tetragonal fluorides K_2CoF_4, $K_2Mg(Co)F_4$, Rb_2CoF_4, and $Rb_2Mg(Co)F_4$. By collating spectral information from all four materials, an unambiguous assignment of the spin-allowed bands has been made, permitting a rational discussion of the significance of the appropriate crystal field parameters.

Theory for $d^{3,7}$ Ions in a Tetragonal Crystal Field. The matrices for the tetragonal field were published by Perumareddi[10] in the strong-field representation, without spin–orbit coupling, and Jesson[11] has made available the complete matrices in the weak-field scheme, both with and without spin–orbit coupling. With the inclusion of spin–orbit coupling, the crystal field matrix factors into two 30 × 30 matrices, transforming as the Γ_6 and Γ_7 representations of the D_{4h}' double group.

Two parameters are required to specify the tetragonal part of the field. Following their definition by Moffitt and Ballhausen,[12] the use of Ds and Dt has become established. In the limit of the point charge formalism, expressions for Dq and Dt may be combined to give the simple relation

$$Dt = {}^4/_7(Dq_{xy} - Dq_z)$$

where Dq_{xy} and Dq_z are the cubic crystal field parameters of the ligands in the xy plane and on the $\pm z$ axis of the octa-

Table I. First-Order Energies for Quartet States of the d^7 Configuration in a Tetragonal Field

	Tetragonal state and energy^a	
$^4T_1{}^b$	$^4A_2{}^b$	$10Dq + 9B - 6Ds + 10Dt$
	$^4E^c$	$10Dq + 9B - {}^{35}/_4Dt$
$^4A_2$	$^4B_1$	$20Dq - 3B - 2Ds + 15Dt$
$^4T_2$	$^4B_2$	$10Dq - 3B - 2Ds + 15Dt$
	$^4E^b$	$10Dq - 3B - 2Ds + {}^{25}/_4Dt$
$^4T_1{}^a$	$^4E^a$	$-3Ds + 5Dt$
	$^4A_2{}^a$	0

^{a} The energy of $^4A_2{}^a$ has been set to zero. If $^4E^a$ is the ground state, then $3Ds - 5Dt$ must be added to each energy.

hedron, respectively. It follows that *Dt* will have the same sign as *Dq* in a tetragonal field of six fluoride ions if there is an axial elongation, and it will have opposite sign if the distortion is an axial compression. This sign convention has been used by most workers, although Perumareddi[10] has used the opposite convention.

The first-order energies for the quartet states are given in Table I. Note that the splitting of the $^4T_{2g}(O_h)$ state depends on *Dt* alone and that of $^4T_{1g}(O_h)$ almost entirely on *Ds*.

It is implicit in our treatment that no effect of the tetragonal field on either the interelectron repulsion energies or the spin–orbit coupling is considered and values of these quantities appropriate to the cubic field case are used in calculations. The prime interest is the investigation of the variation of the energy levels of Co^{2+} with respect to the crystal field parameters *Dq*, *Ds*, and *Dt*.

It is instructive to set the spin–orbit coupling constant to zero to show the behavior of the quartet energy levels as functions of *Ds* and *Dt*. The sensitivity to *Ds* and *Dt* of the state splittings is then easily seen and an appropriate selection of values is shown in Figure 1. We note that the orbital nature of the ground state depends in opposite ways on *Ds* and *Dt*.

The Nature of the Tetragonal Distortion. The compounds of the isostructural series K_2MF_4, Rb_2MF_4 (M = Mg, Zn, Mn, Fe, Co, Ni, Cu) crystallize in the tetragonal space group $D_{4h}{}^{17}$. Complete crystal structures have been determined only in the case of the four compounds K_2MgF_4,[13] K_2NiF_4,[14] K_2CuF_4,[15] and K_2MnF_4[16] and correspond to an axial compression of about 1% in the first three cases and an axial elongation, also about 1%, for K_2MnF_4. It is not possible therefore to make any *a priori* predictions concerning the sense of the tetragonal distortion in Rb_2CoF_4, K_2CoF_4, or Rb_2MgF_4. If the presence of the cobalt ion in the lattice of K_2MgF_4 does not disturb the local structure significantly, the distortion in this host will be one of axial compression.

Experimental Section

K_2CoF_4, Rb_2CoF_4, and $Rb_2Mg(Co)F_4$ were grown by the method given by Birgeneau, *et al.*[17] Crystals of $K_2Mg(Co)F_4$ were grown by slow cooling from a melt containing KF, MgF_2, and CoF_2.

All measurements of absorption spectra were made with a Cary 17 spectrophotometer and matched Glan-Taylor prisms were used in the sample and reference compartments for the polarized spectra. The crystals were cooled by boil-off of liquid helium in a silica flow tube.

Results and Discussion

K_2CoF_4, Rb_2CoF_4, and $Rb_2Mg(Co)F_4$. Spectral Features and Gross Assignments. The absorption spectra in the range 5000–45,000 cm^{-1} were measured at temperatures from 10 to 300 K and for α, σ, and π polarizations. The results are given in Figures 2–4 for σ and π polarizations. The absorption bands are relatively weak and their behavior on cooling, *i.e.*, the narrowing of the bands and the reduction of intensity, is typical of vibronically induced spectra.

In terms of their gross features it is clear that the spectra of K_2CoF_4, Rb_2CoF_4, and $Rb_2Mg(Co)F_4$ are closely related. They show large splittings of the visible band (>1000 cm^{-1}) and high dichroic ratios (up to 7:1), whereas both of these features are much less pronounced for $K_2Mg(Co)F_4$, considered separately below.

Detailed examination of the polarized spectra including the α polarizations shows that the visible bands are electric dipole transitions while the infrared band has significant magnetic dipole character.

From Figure 1 we expect to see transitions to five quartet states, *i.e.*, $^4E_g{}^b$, $^4B_{2g}$, $^4B_{1g}$, $^4E_g{}^c$, and $^4A_g{}^b$. The strong bands in the visible region are obviously the tetragonal components of $^4T_{1g}(O_h)$, split to first order by $|6Ds - {}^5/_4Dt|$. The weak and broad band around 15,000 cm^{-1} in $KCoF_3$[18] ($^4A_{2g}(O_h)$) is not split by the tetragonal field, and, therefore, the correspondingly weak and broad bands in the same region of the spectra of K_2CoF_4, Rb_2CoF_4, and $Rb_2Mg(Co)F_4$ are assigned to the upper state $^4B_{1g}(D_{4h})$. The $^4T_{2g}(O_h)$ state appears not to be split by the tetragonal field and its two tetragonal components $^4E_g{}^b$ and $^4B_{2g}$ are assigned to the broad bands near 7000–7500 cm^{-1}. A summary of some of the relevant spectral data is given in Table II.

From Table I we can obtain estimates of the tetragonal field parameters. The small splitting of the $^4T_{2g}(O_h)$ state means that *Dt* is small and we set an upper limit for $|Dt|$ of 40 cm^{-1}. The splitting between $^4E_g{}^c$ and $^4A_{2g}{}^b$ is then approximately $|6Ds|$. Estimates of *Dq* are obtained from the separation between the infrared band and the broad band assigned to $^4B_{1g}$. The approximate set of parameters is given in Table III.

The Transition to $^4T_{2g}(O_h)$. Transition Mechanism and Selection Rules. There is a considerable amount of fine structure in the band associated with the transitions to the components of $^4T_{2g}(O_h)$ and, from comparisons between α, σ, and π spectra, it is clear that the structure is magnetic dipole in origin. The spectra are shown in Figures 5–7.

In addition to the magnetic dipole fine structure some of the broad-band intensity comes from a vibrationally induced electric dipole mechanism because, as shown in Table II, there

Table II. Positions, Intensities, and Temperature Dependence of Spin-Allowed Bands for Tetragonal Cobalt Fluorides

Cubic and free ion parent		K_2CoF_4			$Rb_2Mg(Co)F_4$			$Rb_2Mg(Co)F_4$ Position
		Position^a	$f_{10}{}^b$	f_{300}/f_{10}	Position	f_{10}	f_{300}/f_{10}	
$^4T_{2g}(^4F)$	α	7,600 ± 50	2.9	1.4	7,400 ± 50	3.3		
	σ	7,500 ± 50	4.6	1.1	7,140 ± 50	5.0	1.1	7,300 ± 50
	π	7,605 ± 30	2.2	1.4	7,400 ± 50	2.4	1.4	7,400 ± 50
$^4A_{2g}$	α, σ, π	15,750 ± 150			14,900 ± 150			15,200 ± 500
$^4T_{1g}(^4P)$	α	20,070 ± 30 20,500 ± 100	22	1.7	19,720 ± 60 20,080 ± 80	24	1.7	
	σ	20,070 ± 30 20,500 ± 100	22	1.75	19,720 ± 60 20,080 ± 80	24		19,800 ± 20 20,200 ± 20
	π	19,120 ± 40	13	1.8	18,115 ± 20	13		18,180 ± 20 18,760 ± 20

^{a} Franck–Condon maxima (cm^{-1}) at 10 K. ^{b} Units of 10^{-6}.

is a temperature-dependent contribution to the oscillator strength and $f_\alpha \neq f_\pi$ at low temperatures.

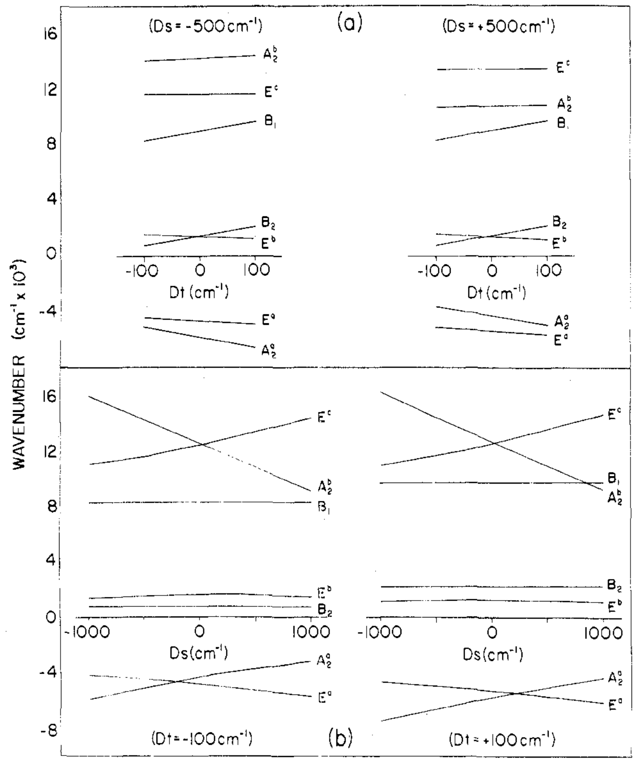

Figure 1. Energies of quartet states of the d^7 configuration in a tetragonal crystal field with zero spin–orbit coupling: (a) $Dq = 750$ cm^{-1}, $Ds = \pm 500$ cm^{-1}; (b) $Dq = 750$ cm^{-1}, $Dt = \pm 100$ cm^{-1}.

Table III. Approximate Crystal Field Parameters (cm^{-1})

	K_2CoF_4	$Rb_2Mg(Co)F_4$	Rb_2CoF_4
Dq	820	765	780
$\lvert Ds \rvert$	200	230	300
$\lvert Dt \rvert$	<40	<40	<40

From Table II we see that the absorption intensity is anisotropic with $f_\sigma/f_\pi \approx 2$. This suggests that this ratio reflects the relative magnetic dipole transition intensities to the orbital degenerate (E) and nondegenerate (B_2) components. If spin–orbit coupling is neglected, it is a simple matter to calculate the magnetic dipole intensity ratios (σ/π) for the alternate ground states $^4A_{2g}$ or $^4E_g{}^a$. These ratios are 0 and 2, respectively, so that this simple model suggests that the ground state is predominantly $^4E_g{}^a$ in character and hence, from Table I, Ds is positive.

Another feature which is apparent from the spectra in Figures 5–7 is that in the series K_2CoF_4, $Rb_2Mg(Co)F_4$, and Rb_2CoF_4 the Franck–Condon maxima of the σ- and π-polarized spectra become increasingly separated, and at the same time there is a large increase of the σ/π intensity ratio in the low-energy tail of the band (see Table IX of ref 19 for D_{4h} and D_{4h}' selection rules). Since the orbital character of the $^4E_g{}^a$ ground state is essentially unaffected through this series, the observations can only be understood if there is an increasing tetragonal splitting of the $^4T_{2g}$ state (increasing $|Dt|$), coupled with an increasing $^4E_g{}^b$ character of the lower energy component. It follows therefore that the $^4B_{2g}$ state lies above $^4E_g{}^b$ and hence Dt is positive and it increases in a corresponding way to the increase of Ds.

These conclusions are based on a simple consideration of the magnetic dipole selection rules in the absence of spin–orbit coupling. It remains to show that a complete (spin–orbit) calculation of magnetic dipole intensities (f_α, f_σ, and f_π) substantiates these conclusions. These were calculated using

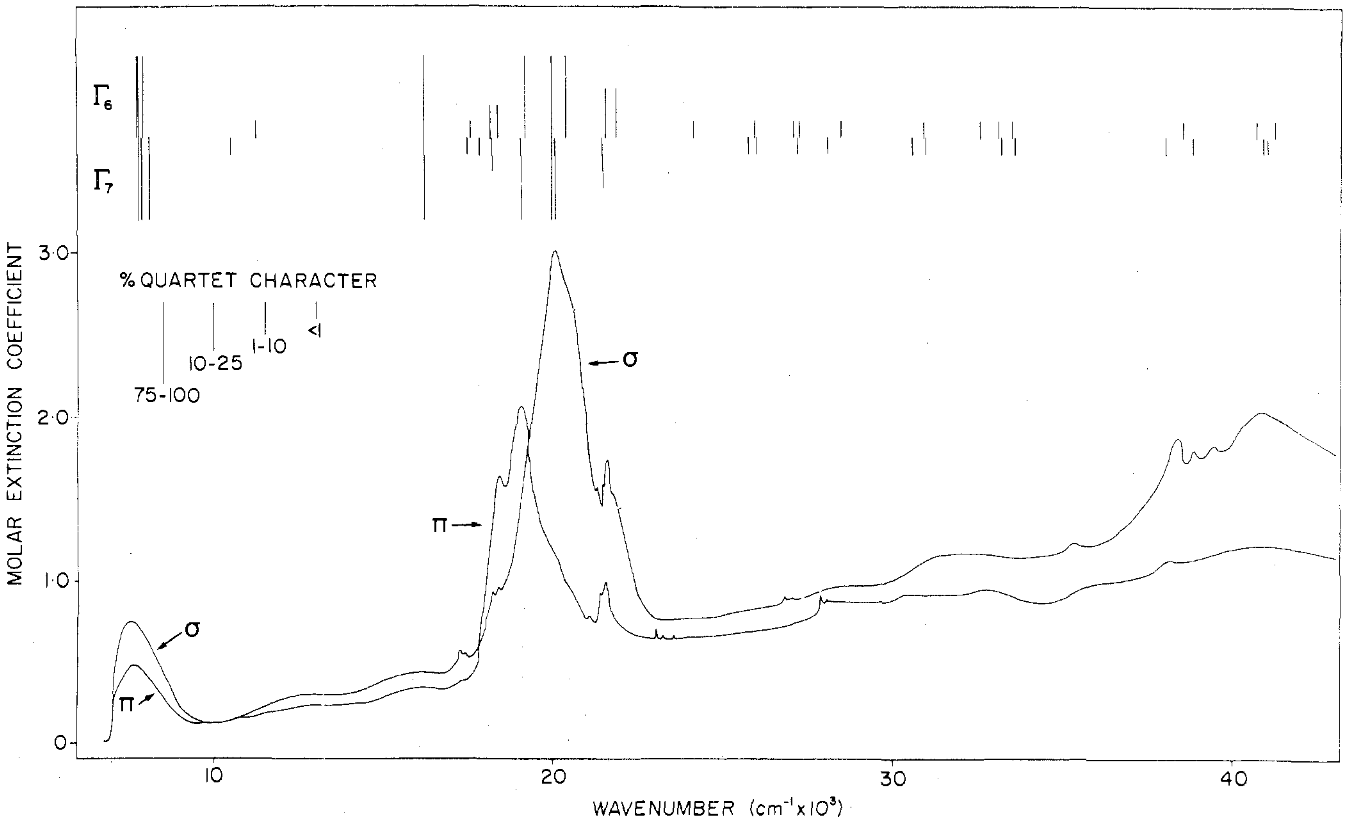

Figure 2. Polarized absorption spectra of K_2CoF_4 and the energy levels, calculated using the parameters $Dq = 825$, $Ds = 195$, $Dt = 10$, and $\zeta = -490$ (all in cm^{-1}). Electron repulsions: $^2G = 16{,}300$, $^4P = 13{,}150$, $^2P = 18{,}950$, $^2H = 20{,}450$, $^2F = 33{,}200$, $^2D = \begin{vmatrix} 44{,}750 & 12{,}700 \\ 12{,}700 & 27{,}100 \end{vmatrix}$ (all in cm^{-1}).

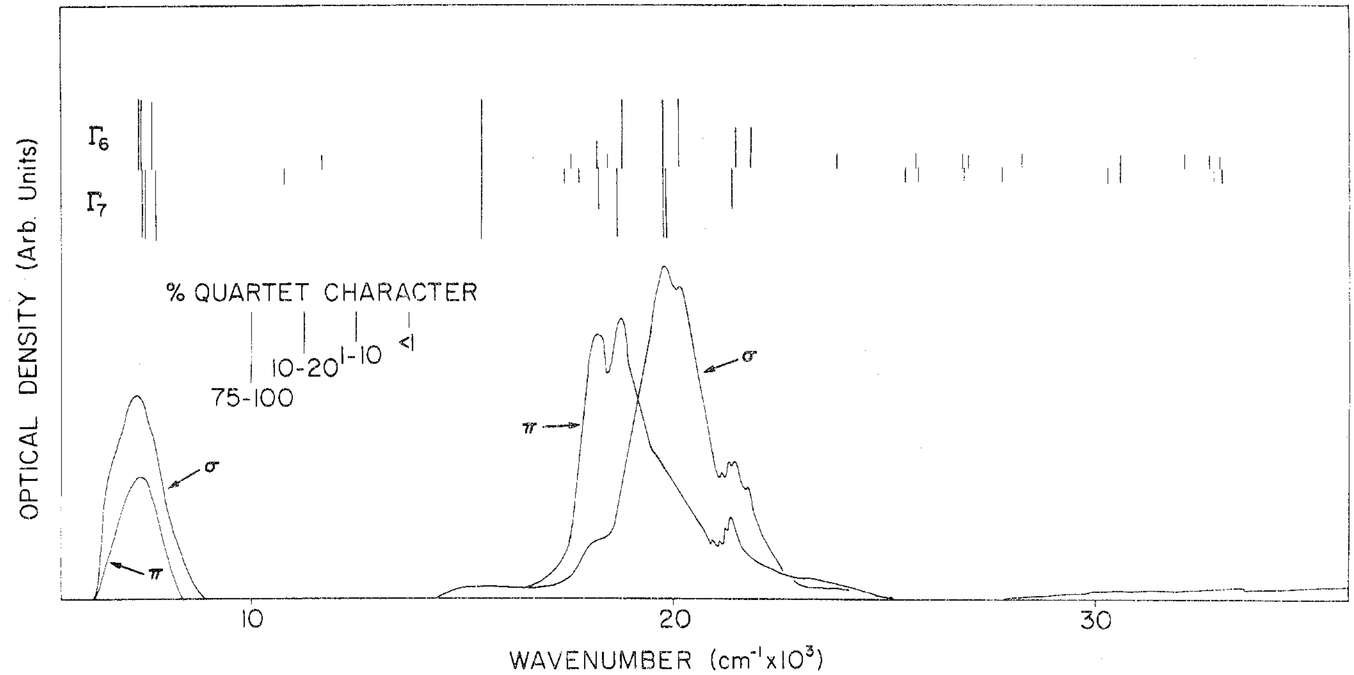

Figure 3. Polarized absorption spectra of $Rb_2Mg(Co)F_4$ and the energy levels calculated using the parameters $Dq = 780$, $Ds = 230$, and $Dt = 20$ (all in cm^{-1}), with the others given in Figure 2.

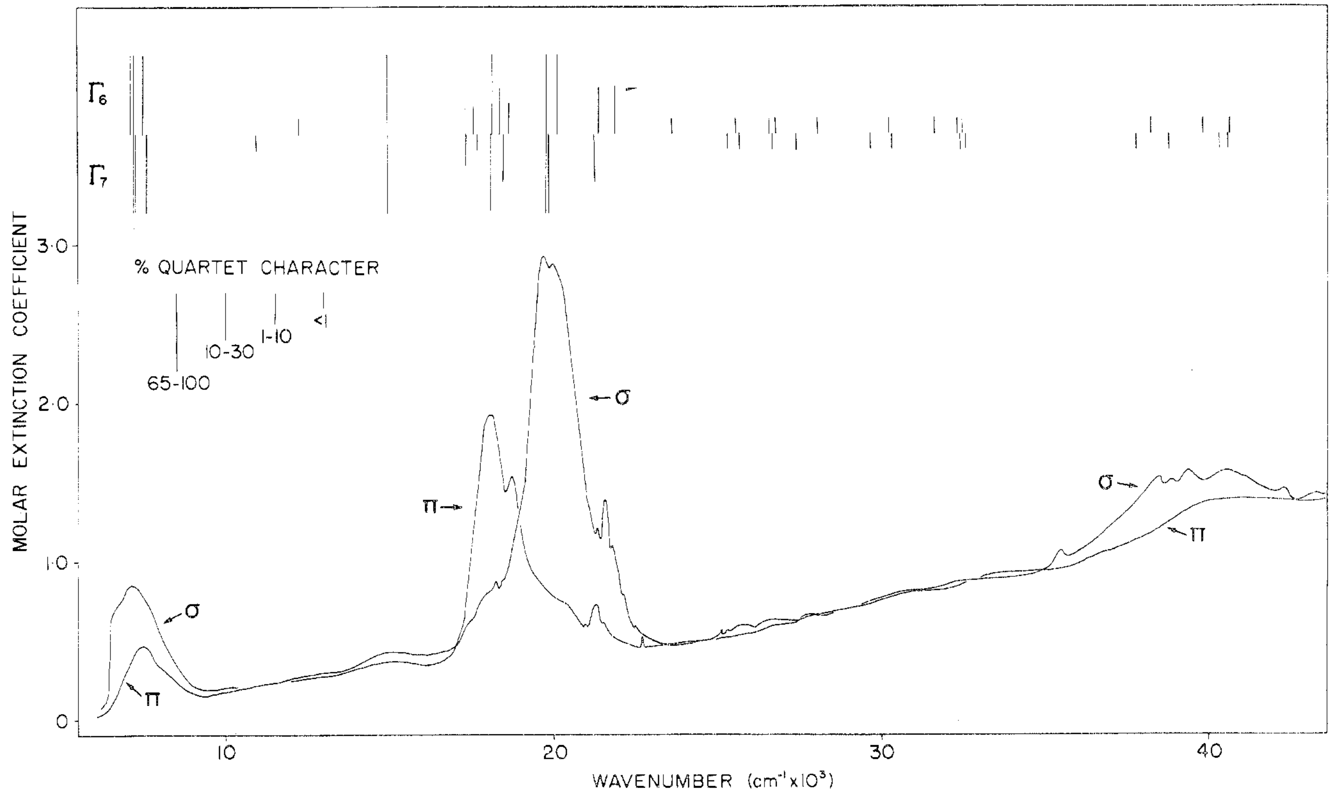

Figure 4. Polarized absorption spectra of Rb_2CoF_4 and the energy levels calculated using the parameters $Dq = 745$, $Ds = 335$, and $Dt = 30$ (all in cm^{-1}), with the others given in Figure 2.

the complete d^7 configuration for the final set of parameters, arrived at below, for the three materials K_2CoF_4, Rb_2CoF_4, and $Rb_2Mg(Co)F_4$. The results are given in Table IV along with the experimental values. It is clear that the experimental oscillator strengths and intensity ratios are dominated by the magnetic dipole contributions and the conclusions reached by the neglect of spin–orbit coupling are correct.

Spin–Orbit Structure. The degenerate Γ_8 spin–orbit components in the cubic field are split in D_{4h}' to give a total of six Kramers doublets for the $^4T_{2g}(O_h)$ state. Three of these belong to Γ_6 and three to Γ_7 of D_{4h}'. Transitions from the Γ_6 ground state should appear in all polarizations for Γ_6 excited states and only in α and π polarizations for Γ_7 excited states. These rules strictly apply only to $Rb_2Mg(Co)F_4$ because detailed analysis of the spectra of the pure materials requires consideration of the magnetic symmetry in the antiferromagnetic phase and we prefer not to consider this complication at the present time.

There are four sharp lines which occur at 6398 cm^{-1} (σ, α, π), 6481 cm^{-1} (σ, α, π), 6766 cm^{-1} (α, π), and 7027 cm^{-1} (α,

π) in the spectrum of $Rb_2Mg(Co)F_4$. These are then assigned to Γ_6, Γ_6, Γ_7, and Γ_7, respectively. Attempts were then made to account for the positions of these lines using the tetragonal spin–orbit matrices. However, although the correct relative ordering of the states can be duplicated, it is impossible to fit their energy spacings with a single set of parameters. As it is known from the work of Sturge[20] the $^4T_{2g}$ state of Co^{2+} is subject to dynamic Jahn–Teller instability and it seems likely that a somewhat analogous situation applies in the present materials. A quantitative understanding will have to await the use of other techniques, such as MCD, not presently available to us.

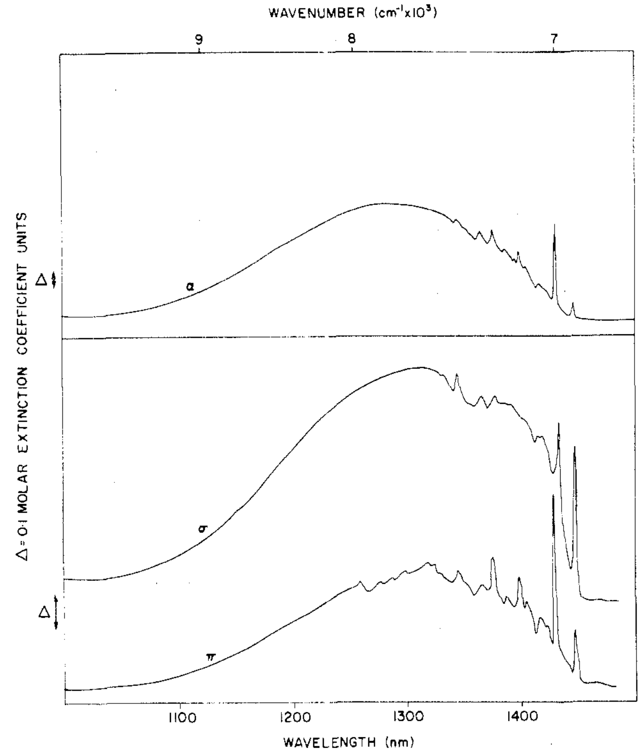

Figure 5. Polarized absorption spectra of K_2CoF_4 in the $^4T_{2g}(O_h)$ region at 30 K (α) and 6.5 K (σ, π).

The polarization ratios of the zero phonon lines contain information about the orbital characters of the excited states associated with each line. We note from Figure 5–7 that the ratio σ/π of the lowest energy pair of lines increases sharply through the series K_2CoF_4, $RbMg(Co)F_4$, and Rb_2CoF_4. Now the magnetic dipole polarization of the transition $^4E_g{}^a \rightarrow {}^4E_g{}^b$ is σ so it follows that $^4E_g{}^b$ lies below $^4B_{2g}$, Dt is positive, and it increases in magnitude through the series, as concluded earlier.

The $^4T_{1g}(^4P)$ Region and Nearby Doublet States. It is apparent from Figures 2–4 that the separation between σ- and π-polarized components increases in the series K_2CoF_4, $Rb_2Mg(Co)F_4$, and Rb_2CoF_4. We can account for this varying separation by using different values of the tetragonal parameter *Ds*, as shown in Figure 8. The value of *Ds* for each case is then fixed by the observed separation.

On closer examination of the spectra in Figure 8 we note the π-polarized main band is made up of two components, whose relative intensities vary through the series K_2CoF_4, $Rb_2Mg(Co)F_4$, and Rb_2CoF_4. This intensity variation can be easily understood by consideration of the spin–orbit coupling between the quartet state and the doublet states which arise from the ^2G term. Examination of the calculated wave functions shows that the quartet–doublet character of the states in this spectral region is very sensitive to the value of the tetragonal field parameter *Ds*. The quartet character changes

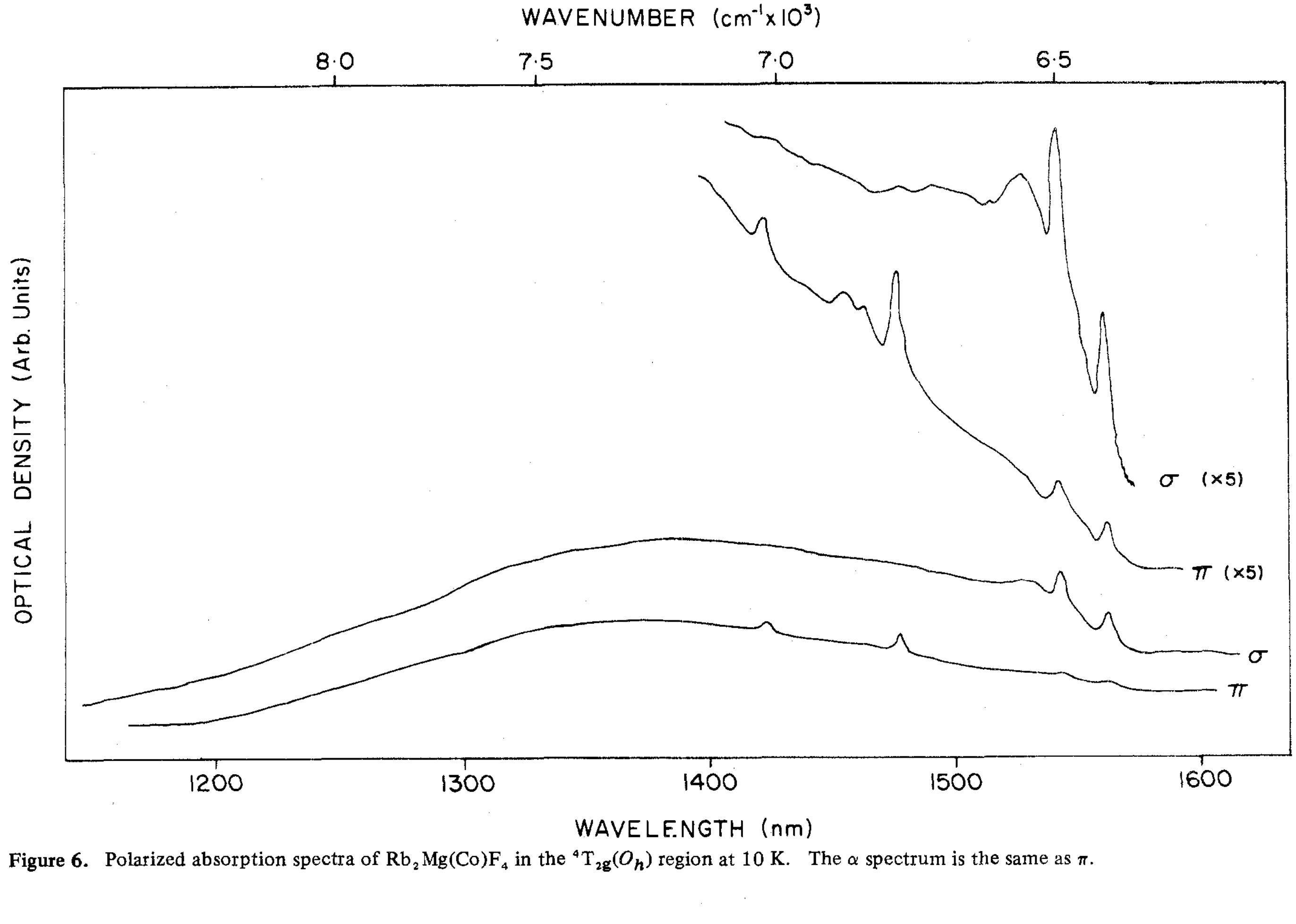

Figure 6. Polarized absorption spectra of $Rb_2Mg(Co)F_4$ in the $^4T_{2g}(O_h)$ region at 10 K. The α spectrum is the same as π.

Table IV. Theoretical Magnetic Dipole Oscillator Strengths[a] of the Transitions to $^4B_{2g}$ and ^4E_g[b]

	Calcd			Obsd		
Material	f_σ	f_π	f_σ/f_π	f_σ	f_π	f_σ/f_π
K_2CoF_4	2.5	1.6	1.60	4.6	2.2	2.1
$Rb_2Mg(Co)F_4$	2.4	1.5	1.62			~2
Rb_2CoF_4	2.4	1.4	1.76	5.0	2.4	2.0

[a] f_σ and f_π in units of 10^{-6}. Calculated using the values of the parameters given in Table V. The refractive index was taken to be unity.

Table V. Crystal Field Parameters for Tetragonal Cobalt Fluorides

	Dq, cm^{-1}	*Ds*, cm^{-1}	*Dt*, cm^{-1}	$\kappa = Ds/Dt$
K_2CoF_4	825 ± 15	195 ± 10	10 ± 5	12–41
$Rb_2Mg(Co)F_4$	780 ± 10	230 ± 10	20 ± 5	9–16
Rb_2CoF_4	745 ± 15	335 ± 20	30 ± 5	9–14

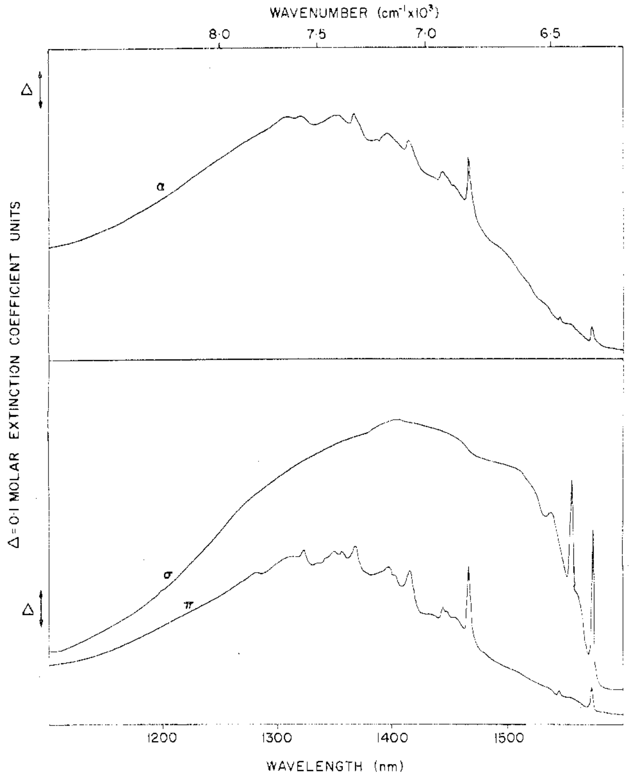

Figure 7. Polarized absorption spectra of Rb_2CoF_4 in the $^4T_{2g}(O_h)$ region at 6 K (α) and 10 K (σ, π).

in the same way as is experimentally observed and this is shown in Figures 2–4 by the vertical lines at the top of each diagram. The positions of the lines give the calculated energies, and the lengths of the lines indicate the approximate amount of quartet character. The crystal field parameters which were used for these calculations are collected in Table V.

The tetragonal components of the ^2P term occur on the high-energy side of the spin-allowed band, in the region near 21,000 cm^{-1}. This relatively narrow absorption band carries between 2 and 5% of the intensity of the spin-allowed band to be compared with a calculated quartet contamination of 7–8% by spin–orbit coupling. It is clear that the intensity of this spin-forbidden band comes from spin–orbit coupling between the doublet and quartet states. The intensity analysis can be taken a step further by examining the polarization of the bands. The highest energy component is $^2P(\Gamma_6)$ and an examination of its wave function shows that the majority of the quartet contaminations come from the σ-polarized quartet states at 20,153 cm^{-1} (70% $^4P_{1/2}$) and 19,776 cm^{-1} (67% $^4P_{3/2}$) rather than the π-polarized state at 18,763 cm^{-1} (18% $^4P_{1/2}$, 6% $^4P_{3/2}$, 70% $^4P_{5/2}$). We expect that the absorption intensity associated with this state will be strongly σ polarized, in agreement with the marked σ polarization of the high-energy side of the band (see Figures 2–4, 8). By a similar analysis the transition to $^2P(\Gamma_7)$, which lies lowest, should be π polarized, in agreement with experiment. The intermediate $^2P(\Gamma_6)$ component should occur in both σ and π polarization, again in agreement with experiment.

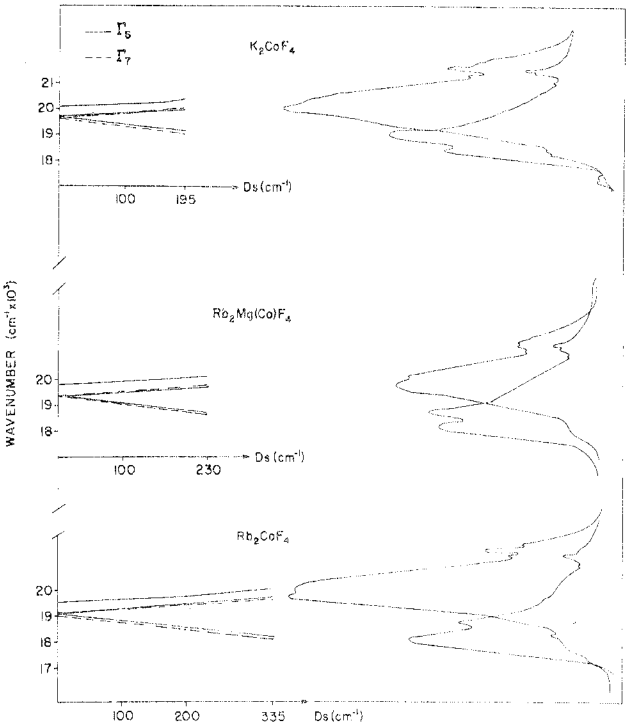

Figure 8. Polarized absorption spectra for the $^4T_{1g}(^4P)$ region. The theoretical fits of the spin-allowed bands to *Ds* are shown on the left.

Crystal Field Parameters for K_2CoF_4, $Rb_2Mg(Co)F_4$, and Rb_2CoF_4. From an analysis of their absorption spectra it has been possible to obtain reasonable precise values for the parameters *Dq*, *Ds*, and *Dt*. The signs of *Ds* and *Dt* have been determined from the spectral information alone and, to our knowledge, this is the first time that a spectral assignment of any tetragonal 3d complex has been made in which assumptions of sign have not been made.

The next step is to see whether the quantities in Table V are physically reasonable. The absolute magnitudes of *Dq* cluster around the value of 775 ± 15 cm^{-1}, obtained for $KCoF_3$, indicating that the environment of the cobalt ion in all of these materials is similar, as expected. Their relative magnitudes are also in the expected inverse order of the respective lattice parameters, where known. Thus, K_2CoF_4 has smaller lattice parameters[4] and therefore a larger *Dq* than Rb_2CoF_4 and it is reasonable to expect that Rb_2MgF_4 has a smaller unit cell (larger *Dq*) than Rb_2CoF_4, just as K_2MgF_4 has a smaller unit cell than K_2CoF_4.[13]

From the definition of $Dq = {}^1/_6 Ze\bar{r}_5{}^4$ it follows that $Dq_z/Dq_{xy} = (x/z)^5$ and if we then define $x/z = 1 + \partial$ we can write

$$Dt = {}^4/_7 Dq_{xy}(1 - (x/z)^5) \approx -{}^4/_7 Dq_{xy}(5\partial)$$

From the values of *Dt* in Table V we calculate that (assuming $Dq_{xy} = 800$ cm^{-1} in each case) $\partial = -0.0044$, -0.0084, and -0.0126 for K_2CoF_4, $Rb_2Mg(Co)F_4$, and Rb_2CoF_4, respectively. This crystal field analysis then leads us to the conclusion that there is a tetragonal elongation of the octahedron in each case ranging from about 0.5% for K_2CoF_4 to just over 1% for Rb_2CoF_4. The magnitudes of these predicted distortions are very similar to the known distortions mentioned

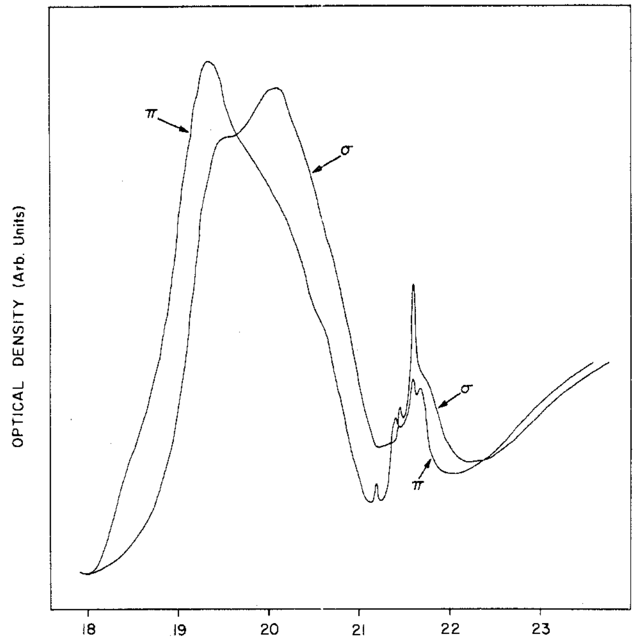

Figure 9. Polarized absorption spectra of $K_2Mg(Co)F_4$ at 10 K for the $^4T_{1g}(^4P)$ region at 10 K.

above. The relative magnitude of the distortions in the two pure materials is supported by the magnetic measurements of Breed, *et al.*,[4] which show that the susceptibility of Rb_2CoF_4 is much more anisotropic than that of K_2CoF_4.

The large positive values of the ratio κ differ from those predicted theoretically, but the difficulties encountered in proposing good radial wave functions can easily account for the difference.

$K_2Mg(Co)F_4$. The absorption spectrum, in the $^4T_{1g}(O_h)$ region, is given in Figure 9 and it can be seen that the anisotropy of the absorption intensity is much less than in the spectra of the other tetragonal fluorides. The separation between the σ- and π-polarized band centers is only about 400 cm^{-1} and we derive an estimate for $|Ds|$ of $\sim$60 cm^{-1}.

Unfortunately, the poor quality and small size of the crystals of $K_2Mg(Co)F_4$ (not grown by H. J. G.) made measurements in the near-infrared region very difficult. However, although the overall broad band could not be measured accurately, we were able to measure the positions and polarizations of five zero phonon lines. They are at 6935 cm^{-1} ($\pi \gg \sigma$), 7010 cm^{-1} (π), 7087 cm^{-1} ($\sigma > \pi$), 7153 cm^{-1} ($\sigma > \pi$), and 7220 cm^{-1} (π).

The polarizations of the two lowest energy lines are highly significant and they are in marked contrast to the polarizations of the analogous lines in the spectra of the other materials. They suggest that *Dt* is negative and therefore of opposite sign to the other cases. We then carried out calculations of the magnetic dipole intensities with the following values of the crystal field parameters: Dq = 800 cm^{-1}, Ds = $\pm$60 cm^{-1}, Dt = $\pm$10 cm^{-1}. The polarization ratio of the lowest (Γ_6) spin–orbit component is not very sensitive to the sign of *Ds* but it is very sensitive to the sign of *Dt*. For Ds = 60 cm^{-1} and Dt = 10 cm^{-1} σ/π = 3.8, while for Ds = -60 cm^{-1} and Dt = -10 cm^{-1} π/σ = 6. The predicted order of spin–orbit states for the latter set of parameters is Γ_6, Γ_7, Γ_6, Γ_6, Γ_7, Γ_7, but the last Γ_7 state carries a vanishing magnetic dipole intensity. The observed polarizations are consistent with the theoretical order of energy levels, but the energy spacings are not in agreement and we conclude that the latter are probably complicated by the dynamic Jahn–Teller effect.

We are unable to define the sign of *Ds* from the experimental data, so we assume that it has the same sign as *Dt*. The sign of *Dt* indicates that the tetragonal distortion is a compression of the octahedron and this conclusion is entirely consistent with the crystal structure of K_2MgF_4.

Concluding Remarks

From the point of view of crystal field theory the materials studied here most closely approach "ideal" systems. The D_{4h} site symmetry is crystallographically exact and all six ligands are similar. It is therefore not too surprising that physically meaningful parameters have been derived from the spectral data. The structure of K_2MgF_4 is known to have an axial compression of the fluoride octahedron and an analysis of the spectrum of Co^{2+} in this material shows that the $CoF_6{}^{4-}$ octahedron has a similar distortion. We note also that a recent analysis[21] of the spectrum of K_2NiF_4 shows that the $NiF_6{}^{4-}$ octahedron has an axial compression, in agreement with the known crystal structure.[14] We therefore have some degree of confidence in the conclusion reached from the analyses of the spectra of K_2CoF_4, $Rb_2Mg(Co)F_4$, and Rb_2CoF_4; *i.e.*, they comprise a class of crystals along with K_2MnF_4, having the K_2MF_4 structure, with axially elongated fluoride octahedra.

"Ideal" though the fluorides are, the assignment of numerical values to the crystal field parameters *Dq*, *Ds*, and *Dt* is not an entirely trivial matter and it requires the use of a great deal of spectral data relating to energies and polarization to reach an unambiguous conclusion. Our treatment differs from other studies in the literature in that no assumptions whatever have been made regarding the signs of either *Ds* or *Dt* (relative to *Dq*). It is usual, for instance, to relate immediately the sign of *Dt* to the sense of the distortion (Dubicki and Day,[22] Perumareddi[23]), but in this work there was no possibility of making such an assumption.

Acknowledgment. We thank K. Y. Wong for use of his computer program for the calculation of the tetragonal magnetic dipole oscillator strength. We also thank Drs. D. J. Breed and A. H. M. Schrama for correspondence relating to the structures of K_2MF_4 crystals.

Registry No. K_2CoF_4, 52873-79-7; Rb_2MgF_4, 52873-80-0; Rb_2CoF_4, 52873-81-1; K_2MgF_4, 52873-82-2.

References and Notes

(1) (a) Research School of Chemistry, Australian National University. (b) Bell Laboratories Inc.
(2) E. Legrand and R. Plumier, *Phys. Status Solidi*, **2**, 317 (1962).
(3) (a) K. G. Srivastava, *Phys. Lett.*, **4**, 55 (1963); (b) E. Legrand and A. van der Bosch, *Solid State Commun.*, **7**, 1191 (1969).
(4) D. J. Breed, K. Gilijamse, and A. R. Miedema, *Physica*, **45**, 205 (1969).
(5) V. J. Folen, J. J. Krebs, and M. Rubenstein, *Solid State Commun.*, **6**, 865 (1968).
(6) C. Bucci, G. Guidi, and C. Vignali, *Solid State Commun.*, **10**, 803 (1972).
(7) C. Bucci and G. Guidi, *Nuovo Cimento B*, **8**, 53 (1972).
(8) J. S. Tiwari, A. Mehra, and K. G. Srivastava, *Phys. Status Solidi*, **28**, 61 (1968).
(9) W. G. Maisch, *J. Appl. Phys.*, **40**, 1330 (1969).
(10) J. R. Perumareddi, *J. Phys. Chem.*, **71**, 3144 (1967).
(11) J. P. Jesson, *J. Chem. Phys.*, **48**, 161 (1968).
(12) W. Moffitt and C. J. Ballhausen, *Annu. Rev. Phys. Chem.*, **7**, 107 (1956).
(13) Y. Yamaguchi, *J. Phys. Soc. Jap.*, **29**, 1163 (1970).
(14) E. P. Maarschall, A. C. Botterman, S. Vega, and A. R. Miedema, *Physica*, **41**, 473 (1969).
(15) K. Knox, *J. Chem. Phys.*, **30**, 991 (1959).
(16) B. O. Loopstra, B. van Laar, and D. J. Breed, *Phys. Lett. A*, **26**, 526 (1968); **27**, 188 (1968).
(17) R. J. Birgeneau, H. J. Guggenheim, and G. Shirane, *Phys. Rev. B*, **1**, 2211 (1970).
(18) J. Ferguson, T. E. Wood, and H. J. Guggenheim, *Aust. J. Chem.*, **25**, 453 (1972).
(19) J. Ferguson, *Progr. Inorg. Chem.*, **12**, 159 (1970).
(20) M. D. Sturge and H. J. Guggenheim, *Phys. Rev. B*, **4**, 2092 (1971).
(21) J. Ferguson, E. R. Krausz, and H. J. Guggenheim, *Mol. Phys.*, in press.
(22) L. Dubicki and P. Day, *Inorg. Chem.*, **10**, 2043 (1971).
(23) J. R. Perumareddi, *Coord. Chem. Rev.*, **4**, 73 (1969).